220GHz High Power Terahertz Wave Generation Based on Miniaturized Vacuum Cerenkov Device

Hai Zhang[1], Jianguo Wang[1, 2], and Changjiang Tong[2]

[1] *School of Electronics and Information Engineering, Xi'an Jiaotong University, Xi'an 710049, China*
[2] *Northwest Institute of Nuclear Technology, Xi'an, 710024, China*
Email: xjtuzhanghai@163.com

***Abstract*—New micromachining techniques now provide the technology to fabricate vacuum electron devices with dimensions suitable for operation in terahertz region. In this paper, results of theoretical and numerical simulation studies of a MW-class, large diameter terahertz wave generator based on the Cerenkov principle are presented. The device consists of a miniaturized foilless diode as well as an oversized rectangular slow wave structure (SWS) which could support surface wave and provide a strong beam-wave coupling. With the method of Particle-in-cell simulation, we investigated the operating characteristics of a prototype 0.22 THz oscillator. It is found that the steady-state, single-frequency operation in the overmoded situation could be realized by the property of surface wave, and the unique voltage tunable capability proves that the device performs as a forward wave oscillator.**

***Keywords*—Overmoded; terahertz source; Cerenkov device; forward surface wave.**

I. INTRODUCTION

Terahertz region is a generic term for the electromagnetic waves within frequencies between 0.1 and 10 THz [1]. In this region, some unique physical phenomena with characteristic features can be produced. However, the development of useful sources for this region presents considerable challenges. Although many advances have been made in the development of solid-state semiconductor lasers and oscillators [2], the potential of traditional vacuum sources such as klystrons, magnetrons and backward wave oscillators, remains virtually untapped. Recent advances in modern micromachining technologies suggested that this was a "natural" route to fabricate small structures, such as cavities, waveguide, and slow wave structures (SWS) which might be used in a scaled-down vacuum electron tubes operating at far greater frequencies [3],[4]. The aim of this paper was to propose a novel compact Cerenkov oscillator at 0.22THz, which might be suitable for mass production and could deliver an output power around MW-Class for potential industrial applications.

In section II, we designed and analyzed a miniaturized electron gun, which could generate a stable and uniform electron beam. In section III, the dispersion relations of the proposed SWS were calculated and the approach for mode selection was also presented. The exactly formulated theory of beam-wave operation near the upper cutoff point was given in section IV, which setup the basically theoretical fundament of the proposed THz device. The simulation investigations were performed in section V, where the results from two different PIC programs were compared to verify the validity of design. Finally, some important conclusions were drawn in section VI.

978-1-4244-2193-0/08/$25.00 ©2008 IEEE

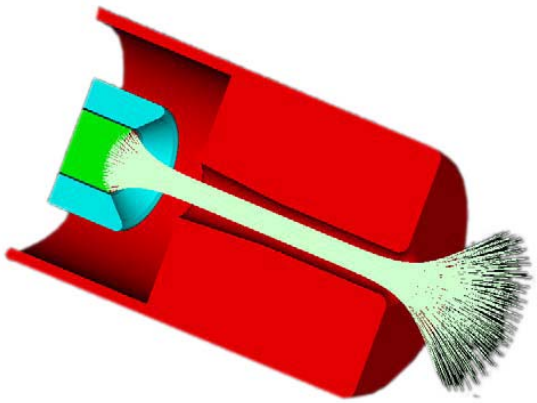

Fig.1 Model of electron gun

II. DESIGN OF VACUUM ELECTRON GUN

A. Operating Principle of Vacuum Cerenkov device

The defining feature of Cerenkov devices is the use of SWS which could provide a set of electromagnetic wave modes with phase velocities less than the speed of light. When the phase velocity of the normal mode of the SWS equals that of the drifting electrons, each electron feels an accelerating or decelerating force, depending on the local phase of the wave. As a consequence, the beam bunches, but there is no net exchange of energy, because equal numbers of electrons speed up and slow down. If the electrons are initially somewhat faster than the wave, however, more electrons are decelerated than accelerated, and a resonant transfer of energy to the wave occurs in addition to the bunching. In this type of so called Cerenkov device, the exchange of energy causes the wave to grow in amplitude, and the bunching enforces the coherence of the radiation. So, one can find that the electron gun and SWS are the two primary components in this kind of devices.

B. Design of Electron Gun: Foilless Diode

The uniform linear electron beam can be produced in a diode which consists of a coaxial transmission line of outer conductor radius R_a, whose centre conductor is truncated to form a cathode. Both the anode (outer conductor) and the cathode can be shaped to vary the beam characteristics. This "foilless diode", as shown is Fig.1, employs a large axial magnetic field to provide insulation and to guide the electrons into a beam [5]. Foilless diodes produce highly annular beams which possess a high current density. Furthermore, the annular beams could have a much higher space-charge-limited current

than the solid beams do, which means that higher current can be generated and transported in a miniaturized vacuum foilless diode with dimensions in the millimetre range.

We investigated the output behaviour of the electron gun by varying the anode radius, while the other parameters keep constant. That is, the cathode radius equals 2.5mm; the drift tube radius equals 3.0mm; the amplitude of incident voltage wave equals 180kV, and the guiding magnetic field is equal to 4.0 Tesla. Fig.2 shows the results of parametric scanning. That is, the total diode voltage after superposition, the beam current, the real beam energy and the equivalent impedance of diode. Each category corresponds to 5 different longitudinal gap distances between cathode and anode, which is defined as S.

III. Design of Overmoded Slow Wave Structure

A. Dispersion Relation of SWS

Dispersion relations, to some extent, are the most important characteristic of SWS. From the diagrams, the operating frequency of device can be approximately determined, and the other eignvalues such as coupling impedance and linear growth rate can also be derived as well. The model of SWS is shown in Fig.3. It is a cylindrical waveguide with the rectangularly corrugated inner wall. The radius of the wave guide (R) is fixed to 3.0mm according to the previous research.

We investigated the dispersion relation of the SWS with various dimensional parameters, and the results are shown in Fig.4. It can be seen that the frequency of interest (0.22THz) is included in the frequency range of the SWS. From the calculated diagrams, we can preliminary determine the values of dimensional parameters of SWS as well as the acceleration voltage of the electron beam in order to ensure the device operate at 0.22THz, i.e., SWS radius (R) equals 3.0mm, SWS period (L) equals 0.4mm, depth of slots (D) equals 2.0mm, width of slot (W) equals 0.2mm, and beam energy is 170keV.

B. Mode Selection

In single mode devices, the dispersion curves for different transverse modes (such as TM_{01}, TM_{02}, TM_{03}) are well separated in frequency, but this issue becomes increasingly complicated when the transverse size of the device becomes larger, because in this overmoded situation the dispersion curves for different transverse modes may overlap in frequency (they are not separated by stop bands), and have the strong interference between each other.

One useful approach for mode selection is to shift the operating point close to the upper edge of pass band (i.e. π point) [6] because when operating in the near π mode, the device could run in a pure surface wave status, where only the lowest mode (TM_{01}) is excited on benefit of the relatively large coupling impedance compared with that of other volumetric wave modes. With this idea, we choose an operating point close to the π point to provide mode selection. Fig.5 shows the dispersion curves of four main competitive modes as well as the electron Doppler line corresponding to 170keV beam energy. It can be seen that the resonant frequency at the operating point noted by 'P' approximately equals 0.22THz in the first Brillion region under this condition.

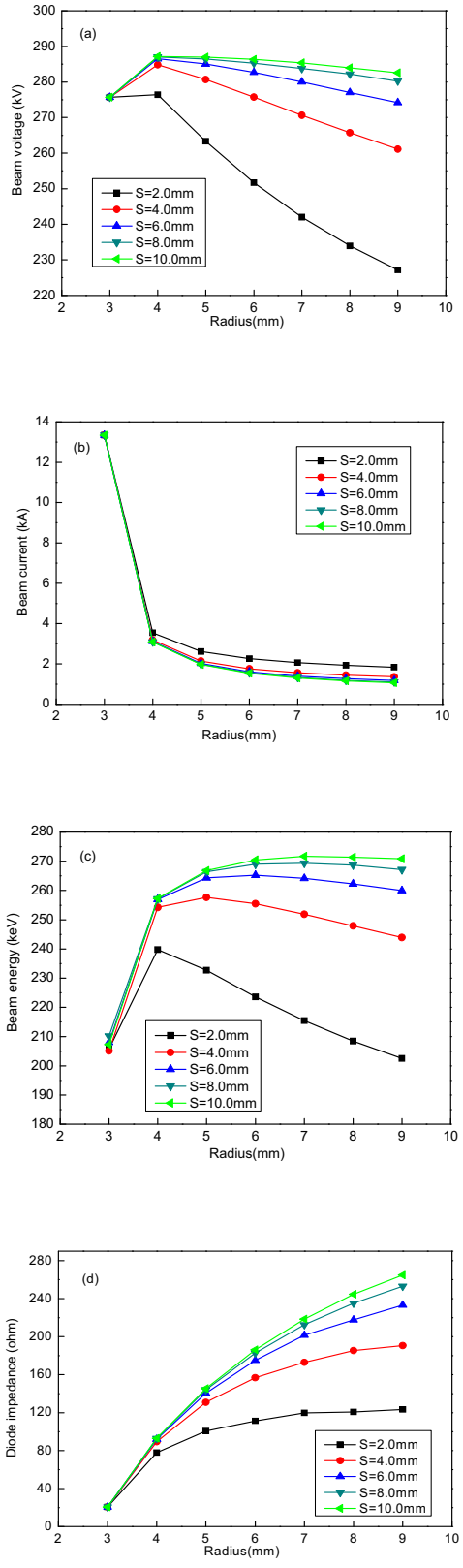

Fig.2 Dependence of output behaviours of electron gun on the anode radius. The four diagrams respectively represent: (a) Total diode voltage, (b) Beam current, (c) Beam energy and (d) Equivalent diode impedance.

IV. Theoretic Analysis of THz Generator Operating near The Upper Cut-off Point

In this section the theoretical model to describe and analyse the Cerenkov oscillator operating near the upper edge of the transmission band, where the group velocity vanishes, is presented. We assume that the beam produces a small space charge field which is proportional to the beam density. The electromagnetic fields in the proposed SWS can be written as:

$$B(x,t)=[B_P(x,k)\varepsilon(z,t)+B_P^{(S)}(x,k)]\ e^{j(kz-\omega t)}+c.c. \quad (1)$$

$$E(x,t)=[E_P(x,k)\varepsilon(z,t)+E_P^{(S)}(x,k)]\ e^{j(kz-\omega t)}+c.c. \quad (2)$$

where, $\varepsilon(z,t)$ is the slowly varying amplitude of the electromagnetic waves, $E_P(x,k)$ and $B_P(x,k)$ are the periodic eigenfunctions of empty SWS, $E_P^{(S)}(x,k)$ and $B_P^{(S)}(x,k)$ are the space charge fields. To determine the equations governing the slowly varying amplitude of the electromagnetic fields, one substitutes (1) and (2) into Maxwell's equations

$$\frac{1}{c}\frac{\partial E}{\partial t}=\nabla\times B-\frac{4\pi}{c}J \quad (3)$$

$$-\frac{1}{c}\frac{\partial B}{\partial t}=\nabla\times E \quad (4)$$

Then one subtracts the dot product of (3) with B_P^* from the dot product of (4) with E_P^*, and then integrates over the volume contained in one period of the structure. Using the periodicity of E_P, $E_P^{(S)}$, B_P and $B_P^{(S)}$, and the boundary condition that the tangential component of the electric field vanishes on the metal wall, the following slowly varying amplitude equation is obtained:

$$\frac{\partial\varepsilon}{\partial t}+v_g\frac{\partial\varepsilon}{\partial z}=-\int dz'\int d^2x_\perp\frac{E_P^*\cdot Je^{-j(kz'-\omega t)}}{U} \quad (5)$$

where the group velocity is shown to be

$$v_g=\frac{c}{4\pi}\int dz'\int d^2x_\perp\hat{z}\cdot\frac{E_P\times B_P^*+E_P^*\times B_P}{U}$$

The normalized energy stored in one period of the structure is given by

$$U=\frac{1}{4\pi}\int dz'\int d^2x_\perp(|E_P|^2+|B_P|^2)$$

When operating far away from the zero group velocity point, as the traditional devices, the dispersion relation of the cold structure can be approximated by a straight line with slope vg, which is constant.

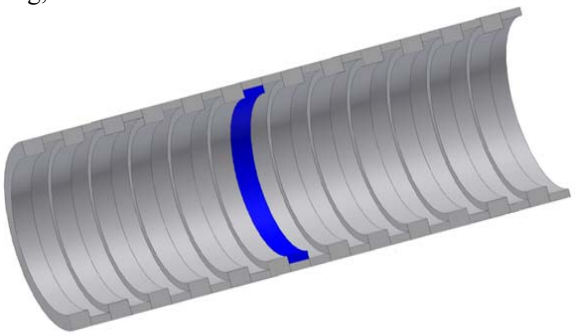

Fig.3 Model of SWS with rectangular rippled inner wall

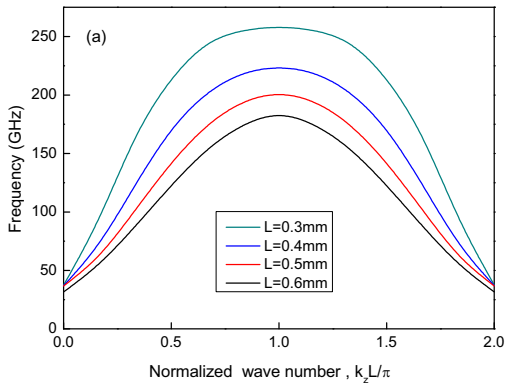

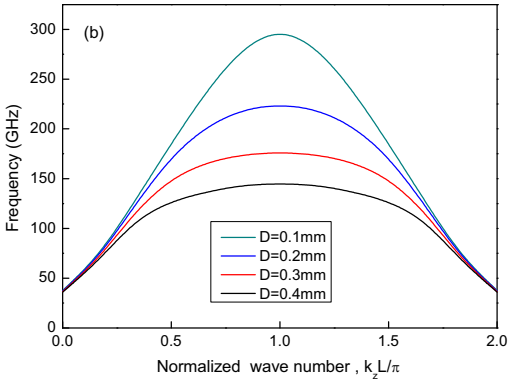

Fig.4 Dispersion diagrams corresponding to different periods of rectangular SWS (a), and different depth of rectangular slots (b).

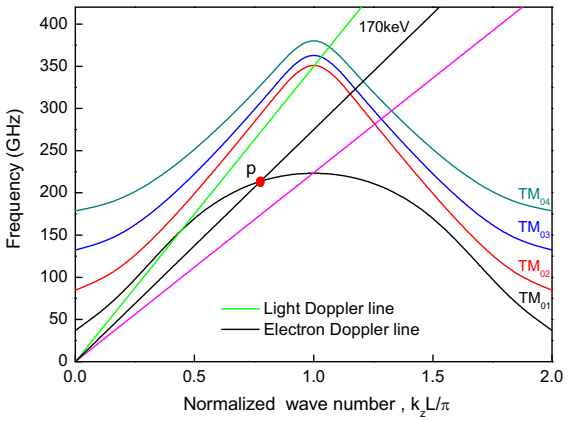

Fig.5 Dispersion diagrams of four competitive modes

However, when operating near the upper edge of the transmission band, like the situation discussed in our paper, the dispersion relation is approximated by quadratic equation:

$$\omega(k)=\omega_0+\frac{1}{2}\frac{\partial v_g}{\partial k}(k-k_0)^2$$

Where, ω_0 and k_0 are the frequency and wave number at the π point. Through a series of very hard and complicated mathematical derivation, the following slowly varying amplitude equation could be obtained.

$$\frac{\partial \varepsilon}{\partial t}+\frac{j}{2}\frac{\partial v_g}{\partial k}\frac{\partial^2 \varepsilon}{\partial z^2}=-\int dz' \int d^2x_\perp \frac{E_P^* \cdot Je^{-j(k_0 z'-\omega_0 t)}}{U} \quad (6)$$

where

$$\frac{\partial v_g}{\partial k}=\frac{c}{4\pi}\int dz' \int d^2x_\perp \hat{z}\cdot\frac{\partial}{\partial k}\frac{E_P\times B_P^*+E_P^*\times B_P}{U}.$$

To solve this equation, the following two boundary conditions are needed:

$$\frac{\partial \varepsilon}{\partial z}(z=0)=jk_{b0}\varepsilon(z=0) \quad (7)$$

$$\frac{\partial \varepsilon}{\partial z}(z=L)=-jk_{b1}\varepsilon(z=L) \quad (8)$$

Where, k_{b0} and k_{b1} are parameters that depend on the coupling of the fields inside and outside the structure. In addition, an electron in the beam is characterized by its phase $\psi=k_0 z-\omega_0 t$ and its energy $mc^2\gamma$, where $\gamma=[1-(v/c)]^{-\frac{1}{2}}$. Therefore, as the beam travels through the interaction region, its phase and energy evolve are according to the following equations:

$$\frac{\partial \psi}{\partial t}+v_z\frac{\partial \psi}{\partial z}=k_0 v_z-\omega_0 \quad (9)$$

$$\frac{\partial \gamma v_z}{\partial t}+v_z\frac{\partial \gamma v_z}{\partial z}=\frac{q}{m}(\varepsilon E_{ZP}+E_{ZP}^{(S)})e^{j(kz-\omega t)}+c.c. \quad (10)$$

Equations (6), (7), (8), (9), and (10) are the analytical model for the device operating near the upper cutoff point, i.e., the "π"point. More detailed mathematical derivation could be found in [7]. In principle it could be used to determine all the quantities which describe the behaviour of the device, such as the operating frequency and its efficiency. However, it needs much more very hard mathematical knowledge and the complicated derivation processes even make the calculation impractical. Therefore, another method, i.e., the particle-in-cell (PIC) simulation is used to investigate the property of the THz device in the next section.

V. PIC Simulation and Results Analysis

The simulation was performed by using the 2.5D full electromagnetic PIC software UNIPIC, which is developed unitedly by the Northwest Institute of Nuclear Technology and Xi'an Jiaotong University, China.

A. Simulation Model of THz Generator

The simulation model of the device is shown in Fig.6. The rectangular rippled-wall SWS is perfect conductors and the z axis performs as the azimuthally symmetric axis. The EM wave at the right end of the structure was truncated by using the convolutional perfectly matched layer [8]. There are no electromagnetic fields in the tube before. The beam is generated by the electron gun in the left side and is injected into the SWS area, where the THz waves are generated. After passing through the SWS, the beam flares to the wall in the end. The operating parameters were set as follows R=3.0mm, L=0.4mm D=0.2mm, and W=0.2mm. Under the conditions of 130kV incident voltage wave and 4.0Tesla magnetic field, the device could work in the steady-state, single-frequency mode.

B. Result Analysis

Fig.7 shows the temporal behaviour of output power of the wave generator as well as the corresponding Fourier transform of the electrical field component at a certain point in the SWS. It can be seen that the signal began to grow up at about 1.0ns, and became saturated at 2.2 ns. After that, the device operated in the steady state at a single frequency of about 0.225THz.

Fig.8 shows the output behaviours of device with various values of the incident voltage wave, resulting in the different beam energy. As the comparisons, the calculations were also performed with software KARAT, which is another famous and reliable PIC simulation program in high power microwave (HPM) fields. It can be found that the output power grown up with the increase of beam voltage, while the oscillating frequency of device is weakly decreased. This phenomenon demonstrates that the operating point of the system is located in the first Brillion region (as shown in Fig.5) and the device does work as a forward wave oscillator.

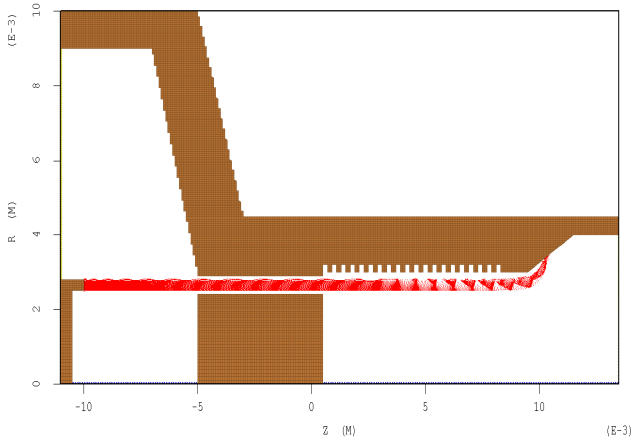

Fig.6 Simulation model of THz Cerenkov generator

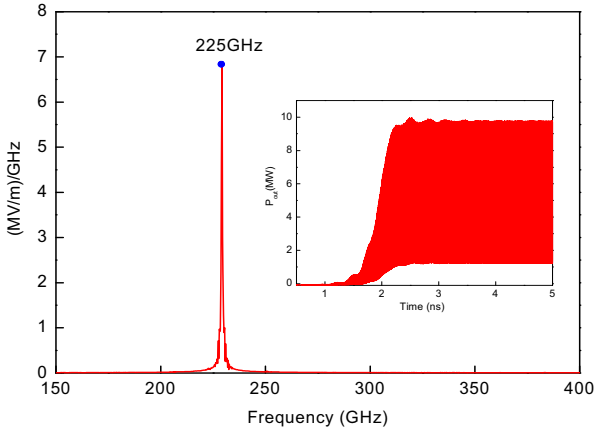

Fig. 7 Fourier spectrum of produced THz signal

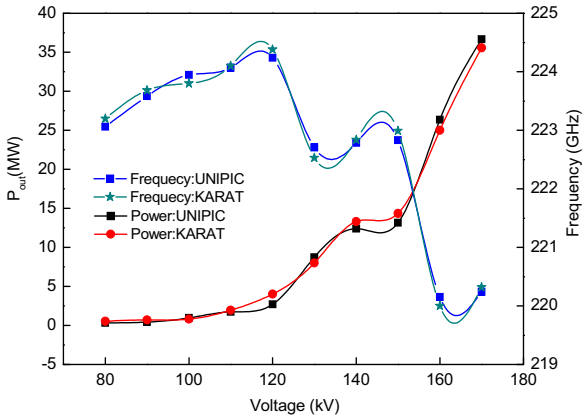

Fig. 8 Dependence of output characteristics of THz generator on the incident voltage wave amplitude

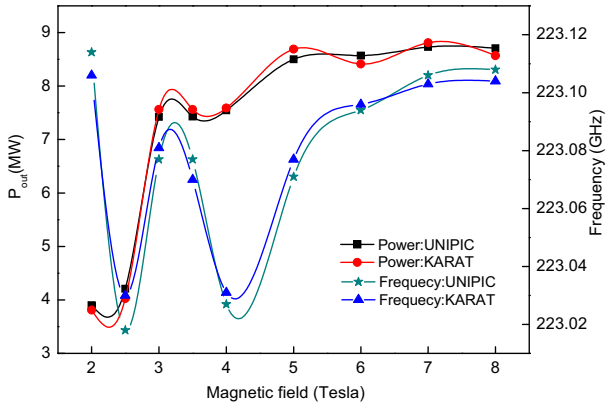

Fig. 9 Dependence of output characteristics of THz generator on the guiding magnetic field

The effect of external applied axial magnetic field on the device behavior is shown in Fig.9. It is obvious that the output power increases with the guiding field, and approach a stable status in the end. It is worth noticing that the system exports relatively small powers in the range of fields below 2.5 Tesla, where the effect of cyclotron resonance appears. To avoid this undesired phenomenon, the magnetic field strength of more than 4.0 Tesla should be employed in the operation.

Furthermore, a distribution pattern of longitudinal electrical field in the device is demonstrated in Fig.10. It can be seen that the field has its maximal value on the surface of SWS (R=3.0mm), and monotonously declines along the radial direction. Meanwhile, the phase of the field alternated a magnitude of about 20π along the Z axis over the length of 20 periods, i.e., 1.0mm<z<9.0mm. These characteristics proved that the device well operated near π point, and possessed the special property of surface wave in TM_{01} mode.

VI. Conclusion

The growing demands of the high power terahertz radiation for the various civil and military applications boost the further

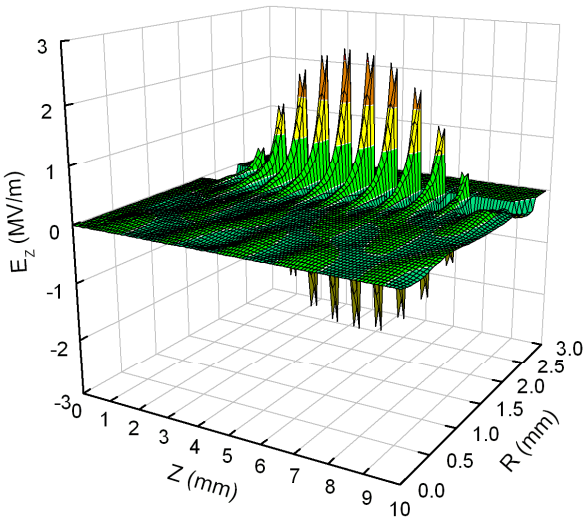

Fig. 10 Axial electrical field distribution in the device

development of conventional HPM devices. In this paper, we presented the theoretical and numerical simulation results of an overmoded, MW class terahertz Cerenkov oscillator. The electron gun was designed and the dispersion property of SWS was also analyzed. It is concluded that the characteristics of surface wave and "π" point operation are crucial to avoid mode competition. It is also found that the device essentially operated as a forward wave oscillator since its operation in the zero order spatial harmonic region. Under the condition of 130kV incident voltage, the output power level above 8 MW was obtained at the frequency of around 0.225THz with perfect time plot and fine spectrum characteristic.

References

[1] D. Dragoman and M. Dragoman, "Terahertz fields and applications," Prog. Quant. Electron., vol. 28, no.1, pp.1-66, February 2004.

[2] T. Taniuchi and H. Nakanishi, "Continuously tunable terahertz wave generation in GaP crystal by collinear difference frequency mixing," Electron. Lett. , vol.40, no.5, pp. 327 – 328, March 2004.

[3] J. Garcia-Garcia, F. Martin, and M. E. Robert, "Optimization of micro machined reflex klystrons for operation at terahertz frequencies," IEEE Trans. Microwave Theory Tech., vol.52, pp. 2366-2370, October 2004.

[4] L. Ives, C. Kory, M. Read, et al., "Development of backward wave oscillators for terahertz applications," in Terahertz for Military and Security Applications, Proc. SPIE, vol.5070, pp.71-82, April 2003.

[5] R. Lawrence Ives, Thuc Bui, John David, Hien Tran, and Michael Read, "Computer Optimization of Electron Gun Designs," in Conference Digest of the Joint 32nd International Conference on Infrared and Millimetre Waves, and 15th International Conference on Terahertz Electronics, vol.1, pp. 152-153, September 2007.

[6] A. N. Vlasov, A. G. Shkvarunets, J. C. Rodgers, et al., "Overmoded GW-Class surface-wave microwave oscillator," IEEE Trans. Plasma. Sci., vol.28, no.3, pp.550-560, June 2000.

[7] S. M. Miller, T. M. Antonsen, B. Levush, and A.Bromborsky, et al, "Theory of relativistic backward wave oscillators operating near cutoff," Phys. Plasmas, vol. 1, no.3, pp.730-740, March 1994.

[8] J. Wang, Y. Wang, and D. Zhang, "Truncation of open boundaries of cylindrical waveguides in 2.5-Dimensional problems by using the convolutional perfectly matched layer", IEEE Trans. Plasma. Sci., vol.34, no.3, pp. 681-690, June 2006.